

The Signature of the Ice Line and Modest Type I Migration in the Observed Exoplanet Mass-Semimajor Axis Distribution

Kevin C. Schlaufman¹ and D. N. C. Lin²

*Astronomy and Astrophysics Department, University of California, Santa Cruz, CA 95064;
kcs@ucolick.org and lin@ucolick.org*

and

S. Ida

*Tokyo Institute of Technology, Ookayama, Meguro-ku, Tokyo 152-8551, Japan;
ida@geo.titech.ac.jp*

ABSTRACT

Existing exoplanet radial velocity surveys are complete in the planetary mass-semimajor axis ($M_p - a$) plane over the range $0.1 \text{ AU} < a < 2.0 \text{ AU}$ where $M_p \gtrsim 100 M_\oplus$. We marginalize over mass in this complete domain of parameter space and demonstrate that the observed a distribution is inconsistent with models of planet formation that use the full Type I migration rate derived from a linear theory and that do not include the effect of the ice line on the disk surface density profile. However, the efficiency of Type I migration can be suppressed by both nonlinear feedback and the barriers introduced by local maxima in the disk pressure distribution, and we confirm that the synthesized $M_p - a$ distribution is compatible with the observed data if we account for both retention of protoplanetary embryos near the ice line and an order-of-magnitude reduction in the efficiency of Type I migration. The validity of these assumption can be checked because they also predict a population of short-period rocky planets with a range of masses comparable to that of the Earth as well as a “desert” in the $M_p - a$ distribution centered around $M_p \sim 30 - 50 M_\oplus$ and $a < 1 \text{ AU}$. We show that the expected “desert” in the $M_p - a$ plane will be discernible by a radial velocity survey with 1 m s^{-1} precision and $n \sim 700$ radial velocity observations of program stars.

Subject headings: planetary systems — planetary systems: formation — planetary systems: protoplanetary disks

¹NSF Graduate Research Fellow

²Kavli Institute of Astronomy and Astrophysics, Peking University, Beijing, China

1. Introduction

Over 200 planets with reliable mass (M_p) and semimajor axis (a) measurements have been discovered around nearby FGK stars in the past decade. At the same time, attempts to build a comprehensive deterministic theory of planet formation have lead to the development of population synthesis models based on the sequential accretion scenario. In Ida & Lin (2004), two of us studied the growth of planetesimals into dynamically isolated embryos as well as their tidal interactions with their parent disks. Using the observed ranges of disk mass, size, and accretion rate we showed that a fraction of embryos evolve into cores with more than a few Earth masses (M_\oplus), accrete massive envelopes, open up gaps near their orbits, and attain asymptotic masses comparable to that of Jupiter. In some massive and persistent disks, the newly formed gas giant planets may migrate toward the proximity of their host stars. In the end these simulations produced the distribution of dynamical and structural properties of planets. Presently, the observed sample of extrasolar planetary properties has become large enough to enable direct comparisons between the theoretically predicted and observed $M_p - a$ distributions that not only delineate the dominant physical mechanisms at work in planet formation, but also provide quantitative constraints on the efficiencies of those processes.

In the latest update of the planet formation models two of us have incorporated the effect of Type I migration (Ida & Lin 2008a). This process is a direct consequence of a protoplanetary core’s tidal interaction with its parent protoplanetary disk. The efficiency of Type I migration was first determined by a linear theory (Goldreich & Tremaine 1980; Ward 1986; Tanaka et al. 2002) that neglected the embryo’s perturbation on the surface density distribution of its parent protoplanetary disk. In the environment of a minimum mass nebula though, this efficiency factor would imply that a protoplanetary embryo with mass a fraction of an Earth mass would migrate from ~ 1 AU into its host star before the severe depletion of the disk gas that is known to occur over a time scale of several Myr. Although this critical mass at which Type I migration causes AU-scale migration on the disk depletion time increases with a , it is still difficult to retain sufficiently massive cores for the onset of dynamical accretion of gas. This argument implies that gas giants should be very rare (Ida & Lin 2008a) and this paradox has led to many in-depth analyses of the Type I migration process. Numerical nonlinear simulations of Type I migration were reviewed by Papaloizou & Terquem (2006) and many potential explanations for slow Type I migration are in the literature: intrinsic turbulence in the disk (Laughlin et al. 2004; Nelson & Papaloizou 2004), self-induced unstable flow (Koller & Li 2004; Li et al. 2005), nonlinear radiative and hydrodynamic feedback (Masset et al. 2006a), and variation in surface density and temperature gradients (Masset et al. 2006b). Dobbs-Dixon (2007) has shown that in some situations the nonlinear Type I migration rate can be less than 10% of the linear prediction.

Another issue studied by two of us (Ida & Lin 2008b, IL hereafter) is the critical embryo mass $M_{crit} >$ at least a few M_{\oplus} required by current models for runaway gas accretion. The embryo is limited by its isolation mass M_{iso} , and the solid surface density profile of the minimum mass solar nebula (MMSN) $\Sigma_d \propto a^{-3/2}$ requires that the M_{iso} scales like $a^{3/4}$. On the other hand, the timescale for growth $\tau_{c,acc}$ scales with $a^{27/10}$. As a result, after the characteristic gas depletion time τ_{dep} the most massive embryos near the ice line have masses $M_c \sim M_{iso} < M_{crit}$. However, since we observe many exoplanets with Jupiter masses at $a \sim 1$ AU, there must be some physical process that is neglected in this simple analysis. Kretke & Lin (2007) outlined one possible solution to this problem in which solids are trapped near regions of the disk where the local pressure requires the gas to rotate with super-Keplerian velocities. When the combined contribution of both Lindblad and corotation resonances are taken into account (Masset et al. 2006b), the migration of protoplanetary cores may be suppressed as well (IL).

In this paper, we utilize the observed data to calibrate the population synthesis models. In §2 we quantitatively show that the existing distribution of exoplanets cannot be explained by models of planet formation that apply the full Type I migration rate predicted from linear theory and that do not include the effects of the ice line. We also point out that the existing observed and synthesized $M_p - a$ distributions are in agreement with each other if we take into account the effect of an ice line barrier and assume a reduction in the magnitude of Type I migration. In addition, we describe the parameters of a radial velocity survey capable of verifying the existence of “desert” in the $M_p - a$ diagram predicted by IL. In §3 we consider the implications of these models and suggest methods to test our assumptions. In §4 we summarize our findings.

2. Analysis

We use the ideas presented in Narayan et al. (2005) and the formalism developed in Cumming (2004) to approximately reproduce the result of Cumming et al. (2008) that showed that the current California and Carnegie Planet Search (CCPS) has announced all planets with orbital period $P < 2000$ days, stellar reflex velocities $K > 20$ m s⁻¹, and eccentricities $e \lesssim 0.6$. In particular, we determine which of the simulated exoplanet systems from IL would be detectable by a radial velocity survey with precision and cadence similar to present-day radial velocity surveys like the CCPS and the High Accuracy Radial Velocity Planetary Search Project (HARPS). In this approach, we combine Equation (26) and (30) of Cumming (2004) and declare that all the synthesized planetary systems from IL with mass $M_p > M_{50}$ where

$$M_{50} \approx \frac{70 M_{\oplus}}{\sqrt{N} \sin i} \left(\frac{\sigma}{\text{m/s}} \right) \left(\frac{P}{\text{yr}} \right)^{1/3} \left(\frac{M_*}{M_{\odot}} \right)^{2/3} \left[\frac{\ln(M/F)}{9.2} \right]^{1/2} \quad (1)$$

are detectable. In Equation (1), N is the number of radial velocity observations, σ is the RMS of spectrograph precision and stellar jitter, i is the inclination of the exoplanet’s orbit, P is the orbital period in years, and M_* is the host stellar mass in solar masses. In the limit of large N , $M \approx 100$ is the number of independent frequencies searched and $F \approx 0.01$ is the false alarm probability – the numerical values are correct to order-of-magnitude and in any case they only very weakly influence our estimate of M_{50} . We note that Equation (1) is formally correct only for single planetary systems in circular orbits; however, Cumming (2004) shows that in the limit of large N Equation (1) applies to multiple planet systems and in the case where $e \lesssim 0.6$. Therefore, we set $M_{50} = \infty$ if $e > 0.6$. We assume a velocity resolution of 1 m s^{-1} .

We then carry out a Monte Carlo simulation in which we assign each of the simulated planetary systems from IL a random host stellar mass, stellar jitter, eccentricity, inclination, and number of radial velocity observations. In this prescription, we use the empirical distributions for host stellar mass, stellar jitter, eccentricity, and number of radial velocity observations given in the updated Butler et al. (2006) catalog¹ of all known exoplanets; we use the standard distribution for random inclinations. We compute which planetary systems have $M_p > M_{50}$ and declare that these systems are detectable in this iteration.

We repeat this process 1000 times. We consider all planetary systems that are detectable according to the M_{50} criterion in 90% of the Monte Carlo iterations robustly detectable. Averaged over host stellar mass, stellar jitter, eccentricity, inclination, and number of radial velocity observations we find that all of the simulated planets from IL in the range $0.1 \text{ AU} < a < 2.0 \text{ AU}$ with

$$M_p \gtrsim \left[174 \left(\frac{a}{\text{au}} \right) + 47 \right] M_{\oplus} \quad (2)$$

are robustly detectable. We include the results of this calculation in Figure 1. The robustly detectable systems are marked with solid circles and we plot the observed $M_p - a$ distribution of known planetary systems as the solid squares.

¹Maintained at <http://www.exoplanets.org>

IL generated a set of 12 realizations of the $M_p - a$ plane under different physical assumptions described in Table 1. One group of models result from disks with the characteristic bump in gas surface density Σ_g due to the coupling effect of the MRI activity and the ice line and with an enhancement in solid surface density Σ_d , another group of models has the bump in Σ_g but not in Σ_d , and the last group ignores the effects the ice line would have on Σ_g and Σ_d . For each group of models, four different parameterizations of the Type I migration rate were used: 100%, 30%, 10%, and 3% of the full rate from linear theory. For each group of models we marginalize the 2D $M_p - a$ distribution of the simulated exoplanet systems in the complete region over planetary mass, leaving us with 1D distributions in semimajor axis. We plot histograms for each group of models: Figure 2 corresponds to the models that disregard the effects of the ice line on Σ_g and Σ_d , Figure 3 corresponds to the models that includes the effect of the ice line on Σ_g but not Σ_d , and Figure 4 corresponds to the models that include the effects of the ice line on Σ_g and Σ_d .

We determine the model that best matches the observed $M_p - a$ distribution in the complete region by computing for each model the p -value distribution that results from comparing 1000 bootstrap resamplings from that model in the complete region with 1000 resamplings of the observed data in the complete region. We include the results of this calculation in Figure 5 and we also report median p -values and 95% intervals in the last three columns of Table 1. We find that only models that include the effects of the ice line on both the gas and solid surface density of the disk and apply a Type I migration rate an order-of-magnitude less than that predicted by linear theory (models C01C and C003C) are consistent with the observed data in the complete region. Models which neglect the presence of the ice-line barrier generally do not yield the observed up-turn in the period distribution of the known planets and are rejected at very high confidence. Models with efficient Type I migration generally under predict the fraction of stars with detectable gas giants, especially for those with a outside the ice line. Therefore, we argue that the population synthesis models presented in IL incorporating a Type I migration rate much reduced from linear theory and the effects of the ice line on both the solid and gas surface densities (Σ_d and Σ_g respectively) are at least plausible deterministic models for giant planet formation. We also note that the observed data suggests that the ad hoc prescription for the location of the ice line used by IL underestimates its radius by perhaps even a factor of two.

Furthermore, in the presentation of their population synthesis models IL illustrated the presence of a “desert” in the $M_p - a$ distribution. This sparsely populated region is depleted due to both Type I migration and runaway gas accretion. For Models C01C and C003C, this “desert” is centered around $M_p \sim 30 M_\oplus$ and $a < 1$ AU. We use the same detection strategy described above, only now we model the number of radial velocity observations of each planetary system over a period of about ten years as a Gaussian random variable with

mean μ_n and standard deviation σ_n ; we round each random deviate to the nearest whole number. We then fit a two component Gaussian mixture model to the $M_p - a$ distribution of all robustly detected planet with mass $M_p < 100 M_\oplus$, and we say the “desert” is detected if the mean vectors of the two Gaussians are offset by more than 0.6 in $\log a$ and the minor axis of the Gaussian at smaller orbital radius is larger than the minor axis of the Gaussian at larger orbital radius. In other words, if the two components of the mixture model bracket the corner of a region devoid of extrasolar planets – a metaphorical “desert” – we say the “desert” is resolved. We find that when $\mu_n = 700$ and $\sigma_n = 50$, the two components of the mixture model bracket a barren region and therefore the “desert” is resolved more than 90% of the time. We illustrate results of our calculation in Figure 6. As a result, a radial velocity campaign with the parameters described above will be able to confirm the fidelity of the models presented in IL.

3. Discussion

The key prediction of IL is that for masses at which the dominant migration mechanism is Type I migration – $M_p \lesssim 50 M_\oplus$ – there will be a dearth of exoplanets within 1 AU of their host stars, simply because the timescale for Type I migration is so much shorter than the disk dispersal time. Since they are formed interior to the ice line, these planets are likely to be rocky and have mass a few M_\oplus . IL also predict an overdensity of gas giant planets at ~ 2 AU resulting from the ice line. We show in Figure 6 that one can quantitatively detect these features in the observed $M_p - a$ with a radial velocity survey with 1 m s^{-1} precision and about 700 radial velocity observations, or about ten years worth of data from the Automated Planet Finder (APF). In future work, we will examine the ability of missions like the Space Interferometry Mission (SIM) to verify the same features in $M_p - a$ plane.

In addition to the upper and lower M_p bound, the “desert” is also surrounded by populated domains in the a distribution. While the ice line provides a strong up-turn at a few AU, the models by IL also imply a large population of short-period rocky planets as a consequence of Type I migration. Despite an order-of-magnitude decrement in the efficiency of Type I migration, the simulated $M_p - a$ distribution of models C01C and C003C indicate that in the proximity of their host stars, rocky planets with $M_p \sim$ a few M_\oplus are at least an order-of-magnitude more common than close-in gas giants (see Figure 6 of IL). Other authors have already pointed out the observational difficulties inherent in the search for this population of “super-Earths” through radial velocity observations (Narayan et al. 2005). Finally, we note that the models of IL did not include dynamical interactions between planets in multiple planetary systems, and these interactions can broaden the simulated a distribu-

tion and eccentricity distribution. We will include these effects in future generations of the population synthesis models.

4. Conclusion

We used the fact that existing exoplanet radial velocity surveys are complete in the planetary mass-semimajor axis ($M_p - a$) plane where $0.1 \text{ AU} < a < 2.0 \text{ AU}$ and M_p is in the range specified by Equation (2) to show that the observed semimajor axis distribution in the complete region cannot be explained by models of planet formation that use the full Type I migration rate predicted by linear theory and that do not include the effects of the ice line. Moreover, we also demonstrated that the expected “desert” in the $M_p - a$ plane at about $M_p \sim 30 M_\oplus$ and $a < 1 \text{ AU}$ predicted by IL will be discernible by a radial velocity survey with 1 m s^{-1} precision and $n \sim 700$ radial velocity observations of program stars. Such an observational campaign will also verify the predicted inner boundary of the “desert” where we expect a large population of super-Earths have migrated to and halted in the proximity of their host stars.

We thank A. Cumming, G. Laughlin, G. Marcy, and Michel Mayor for useful conversation and the anonymous referee for some insightful comments. This research has made use of NASA’s Astrophysics Data System Bibliographic Services. This material is based upon work supported under a National Science Foundation Graduate Research Fellowship, NASA (NAGS5-11779, NNG06-GF45G, NNX07A-L13G, NNX07AI88G), JPL (1270927), NSF(AST-0507424), and JSPS.

REFERENCES

- Butler, R. P., et al. 2006, *ApJ*, 646, 505
- Cumming, A. 2004, *MNRAS*, 354, 1165
- Cumming, A., Butler, R. P., Marcy, G. W., Vogt, S. S., Wright, J. T., & Fischer, D. A. 2008, *PASP*, 120, 531
- Dobbs-Dixon, I. M. 2007, Ph.D. Thesis
- Goldreich, P., & Tremaine, S. 1980, *ApJ*, 241, 425
- Ida, S., & Lin, D. N. C. 2004, *ApJ*, 604, 388

- Ida, S., & Lin, D. N. C. 2008, *ApJ*, 673, 487
- Ida, S., & Lin, D. N. C. 2008, ArXiv e-prints, 802, arXiv:0802.1114
- Laughlin, G., Steinacker, A., & Adams, F. C. 2004, *ApJ*, 608, 489
- Li, H., Li, S., Koller, J., Wendroff, B. B., Liska, R., Orban, C. M., Liang, E. P. T., & Lin, D. N. C. 2005, *ApJ*, 624, 1003
- Koller, J., & Li, H. 2004, *The Search for Other Worlds*, 713, 63
- Kretke, K. A., & Lin, D. N. C. 2007, *ApJ*, 664, L55
- Masset, F. S., D’Angelo, G., & Kley, W. 2006, *ApJ*, 652, 730
- Masset, F. S., Morbidelli, A., Crida, A., & Ferreira, J. 2006, *ApJ*, 642, 478
- Narayan, R., Cumming, A., & Lin, D. N. C. 2005, *ApJ*, 620, 1002
- Nelson, R. P., & Papaloizou, J. C. B. 2004, *MNRAS*, 350, 849
- Papaloizou, J. C. B., & Terquem, C. 2006, *Reports of Progress in Physics*, 69, 119
- Tanaka, H., Takeuchi, T., & Ward, W. R. 2002, *ApJ*, 565, 1257
- Ward, W. R. 1986, *Icarus*, 67, 164

Table 1. Model Descriptions from Ida & Lin (2008b)

Name	C_1^a	Σ_g Enhanced	Σ_d Enhanced	p_L^b	\bar{p}^c	p_U^d
C1C	1	Yes	Yes	6.9×10^{-6}	2.8×10^{-3}	1.7×10^{-1}
C03C	0.3	Yes	Yes	1.6×10^{-6}	1.7×10^{-3}	1.2×10^{-1}
C01C	0.1	Yes	Yes	9.9×10^{-3}	8.6×10^{-2}	7.2×10^{-1}
C003C	0.03	Yes	Yes	3.2×10^{-3}	6.0×10^{-2}	6.0×10^{-1}
C1B	1	Yes	No	2.9×10^{-12}	7.3×10^{-8}	9.6×10^{-5}
C03B	0.3	Yes	No	5.8×10^{-9}	1.4×10^{-5}	2.8×10^{-3}
C01B	0.1	Yes	No	3.4×10^{-6}	2.8×10^{-3}	2.2×10^{-1}
C003B	0.03	Yes	No	5.1×10^{-5}	1.2×10^{-2}	3.8×10^{-1}
C1_p4	1	No	No	1.0×10^{-16}	1.0×10^{-16}	1.0×10^{-16}
C03_p4	0.3	No	No	1.0×10^{-16}	1.0×10^{-16}	1.0×10^{-16}
C01_p4	0.1	No	No	1.0×10^{-16}	1.0×10^{-16}	1.0×10^{-16}
C003_p4	0.03	No	No	4.4×10^{-16}	2.2×10^{-11}	3.6×10^{-7}

^aFrom Ida & Lin (2008b) – C_1 equivalent to the fraction of the full Type I migration rate predicted from linear theory applied during the simulation

^blower bound of an interval centered on median p -value which contains 95% of our bootstrap realizations

^cMedian p -value of our bootstrap realizations

^dUpper bound of an interval centered on median p -value which contains 95% of our bootstrap realizations

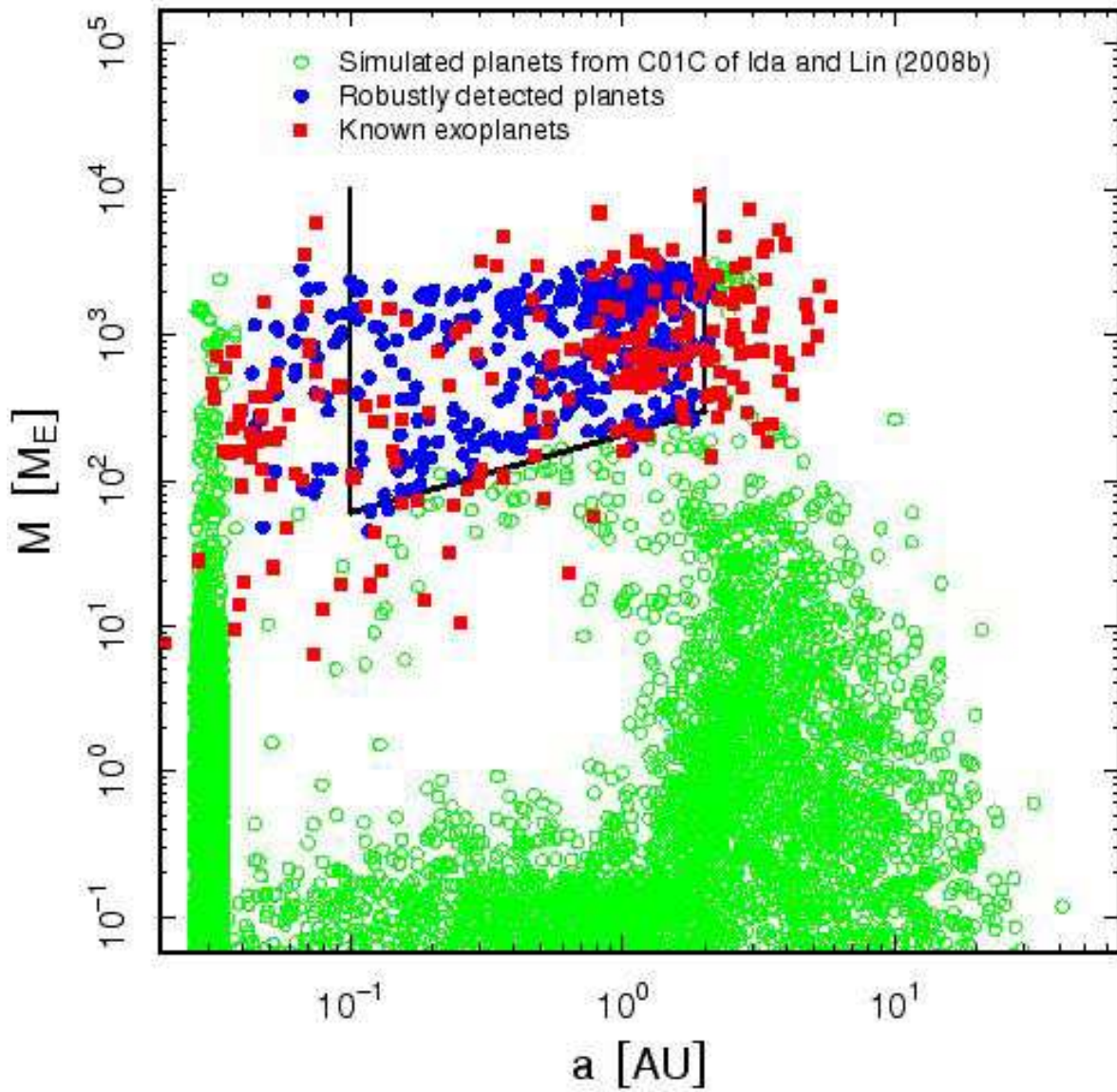


Fig. 1.— Results of our Monte Carlo simulation. The open circles are the simulated planets from Figure 3 of Ida & Lin (2008b); the model includes the effects of the snow line on the surface density of gas Σ_g and dust Σ_d . The Type I migration rate in the simulation is 0.1 times the prediction from linear theory. The filled circles are planets that are robustly detected, that is, planets that would be detected at least 90% of the time by current radial velocity surveys. We also plot all known exoplanet planets as filled squares. All simulated planets in the range $0.1 \text{ AU} < a < 2.0 \text{ AU}$ with M_p as specified by Equation (2) denoted by the heavy black lines are robustly detected, so existing radial velocity surveys are complete in that range. See the electronic edition of the Journal for a color version of this figure.

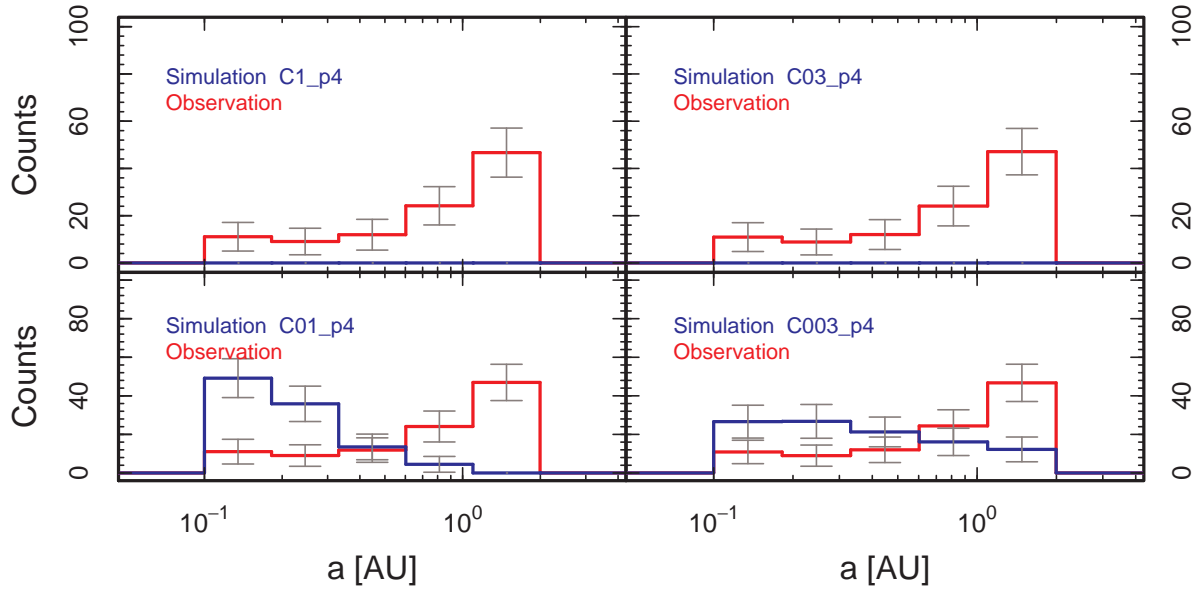


Fig. 2.— 1D distribution in semimajor axis derived from the projection of the 2D distribution in the complete region of the $M_p - a$ plane from Ida & Lin (2008b) for the disks without the bump in Σ_g or Σ_d . The upper left panel uses the full Type I migration rate from linear theory, the upper right panel uses 30% of the full rate, the bottom left panel uses 10% of the full rate, and the bottom right panel uses 3% of the full rate. See the electronic edition of the Journal for a color version of this figure.

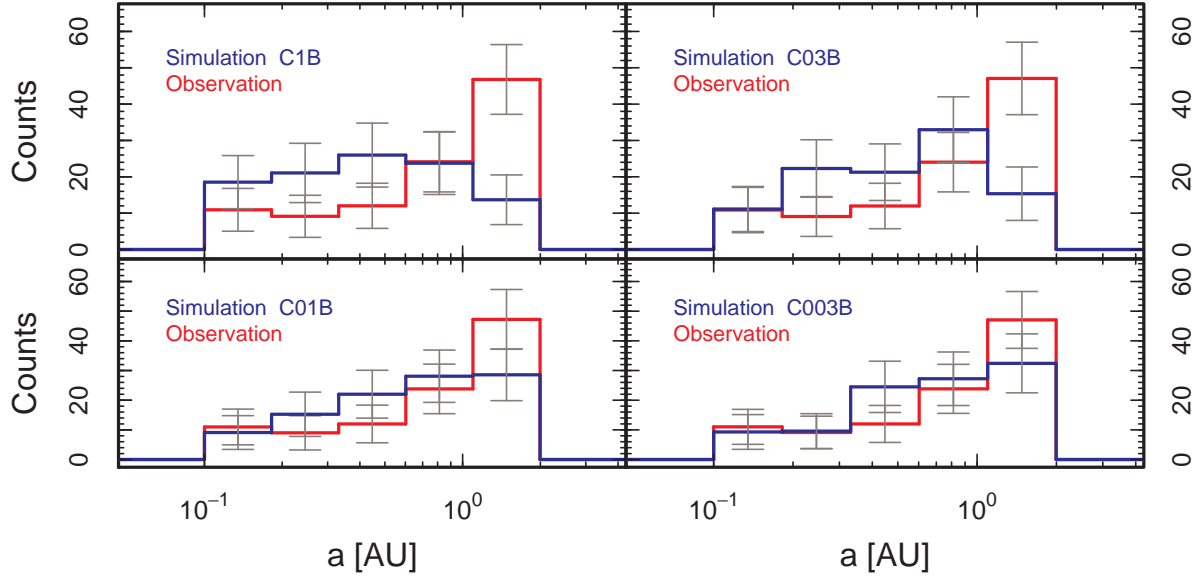


Fig. 3.— 1D distribution in semimajor axis derived from the projection of the 2D distribution in the complete region of the M_p – a plane from Ida & Lin (2008b) for the disks with the bump in Σ_g but without enhancement in Σ_d . The upper left panel uses the full Type I migration rate from linear theory, the upper right panel uses 30% of the full rate, the bottom left panel uses 10% of the full rate, and the bottom right panel uses 3% of the full rate. The error bars indicate the $2\text{-}\sigma$ region. See the electronic edition of the Journal for a color version of this figure.

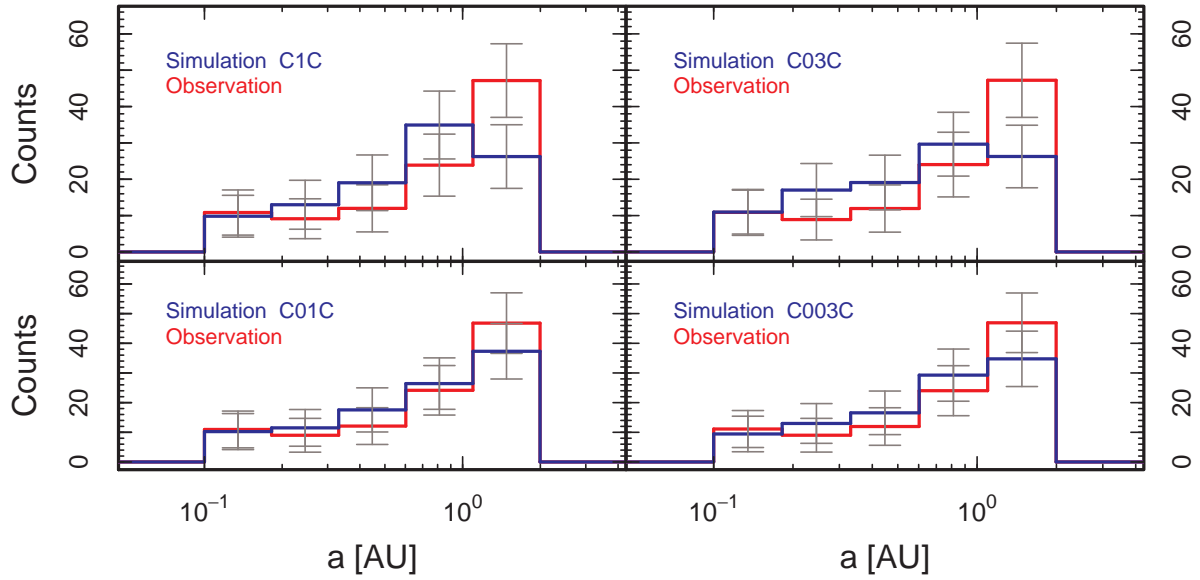


Fig. 4.— 1D distribution in semimajor axis derived from the projection of the 2D distribution in the complete region of the $M_p - a$ plane from Ida & Lin (2008b) for the disks with the bump in both Σ_g and Σ_d . The upper left panel uses the full Type I migration rate from linear theory, the upper right panel uses 30% of the full rate, the bottom left panel uses 10% of the full rate, and the bottom right panel uses 3% of the full rate. The error bars indicate the $2\text{-}\sigma$ region. See the electronic edition of the Journal for a color version of this figure.

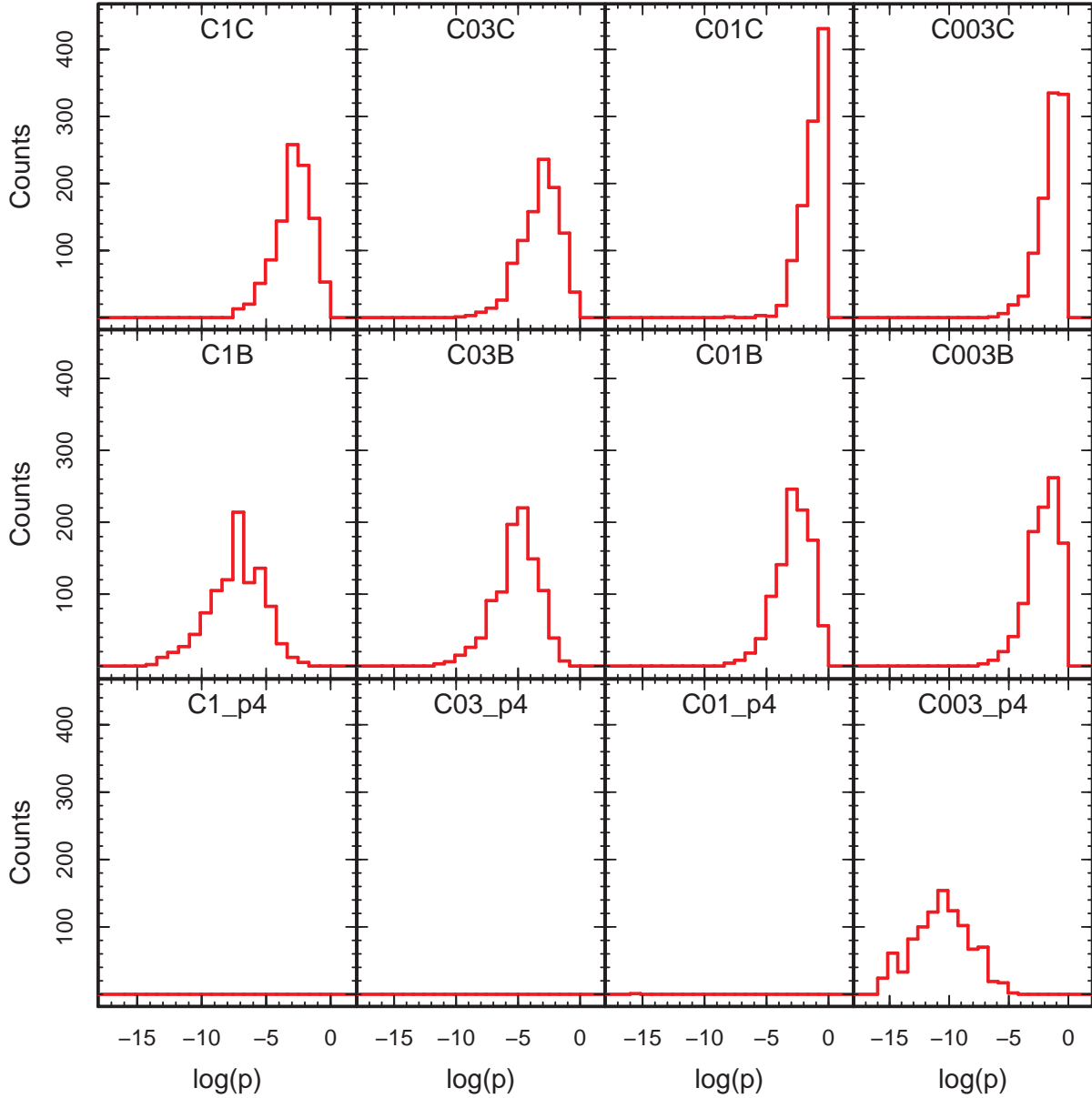


Fig. 5.— Distribution of the Kolmogorov-Smirnov test p -values resulting from 1000 bootstrap resamplings; similar distributions will have a sharply-peaked p -value distributions with a maximum near $p \sim 1 \Rightarrow \log p \sim 0$. The top row shows the results for models including the bump in both Σ_g and Σ_d , the middle row shows models including just the bump in Σ_g , and the bottom row shows models with no bump in Σ_g or Σ_d . For all rows, the first column shows models with the full Type I migration rate, the second column shows models with 30% of the full Type I migration rate, the third column shows models with 10% of the full Type I migration rate, and the fourth column shows models with 3% of the full Type I migration rate. The p -value distribution of the model with the bump in both Σ_g and Σ_d and 10% of the full Type I migration rate is the best match to the observed data. There are no histograms for models C1-p4, C03-p4, or C01-p4 because the p -values were vanishingly small. See the electronic edition of the Journal for a color version of this figure.

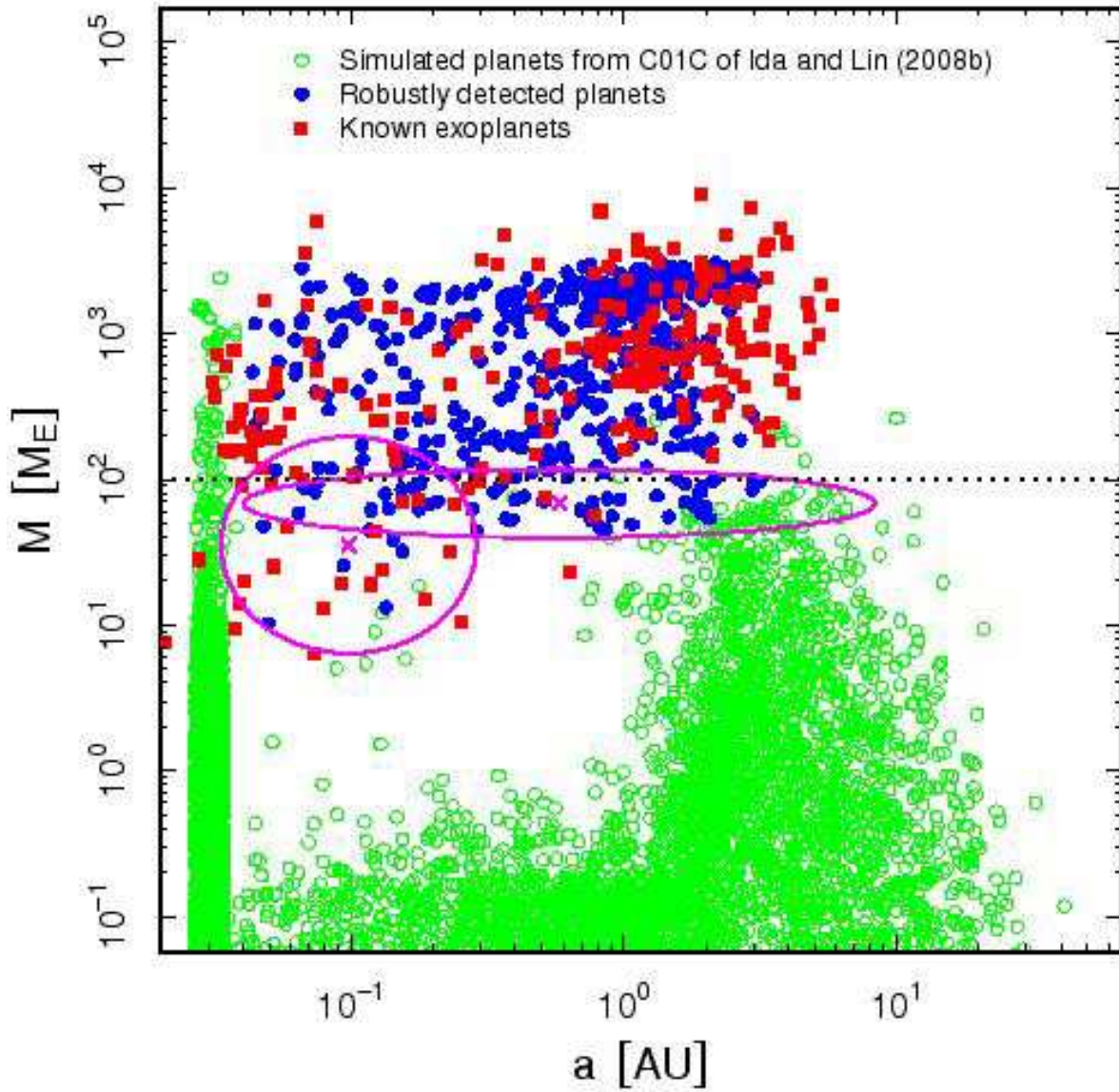


Fig. 6.— Results of our Monte Carlo simulation. The open circles are the simulated planets of model C01C. As in Figure 1, the filled circles are planets that are robustly detected by a radial velocity survey with $n \sim 700$ observations per program star; we plot all known exoplanet planets as filled squares. The centers of the best fit Gaussian mixture to all robustly detected exoplanets below the dashed line at $100 M_{\oplus}$ models are marked by the two X’s, while the characteristic ellipses of each component are the solid lines. We say the “desert” is detected if the mean vectors of the two components are offset by more than 0.6 in $\log a$ and the minor axis of the ellipse at small orbital radius is larger than the minor axis of the ellipse at large orbital radius. We find that the “desert” is detected more than 90% of the time when $\mu_n = 700$. See the electronic edition of the Journal for a color version of this figure.